Earth and Planetary Science Letters 146 (1997) 659–675

EPSL

A U–Pb age from the Toarcian (Lower Jurassic) and its use for time scale calibration through error analysis of biochronologic dating

József Pálfy [a,*], Randall R. Parrish [b,1], Paul L. Smith [a,2]

[a] Department of Earth and Ocean Sciences, University of British Columbia, 6339 Stores Road, Vancouver, B.C., V6T 1Z4, Canada
[b] Geological Survey of Canada, 601 Booth Street, Ottawa, Ont., K1A 0E8, Canada

Received 26 July 1996; accepted 2 December 1996

Abstract

The Early Jurassic is the most poorly constrained part of the geochronologic scale within the Mesozoic, owing to the scarcity of calibration points. We report a new U–Pb zircon age of 181.4 ± 1.2 Ma (2σ) from an ash layer within the type section of Crassicosta Zone, a North American regional standard ammonite zone in the Middle Toarcian. For time scale calibration, the isotopically dated level needs to be tied to the Jurassic chronostratigraphic framework established in northwest European successions. Three major contributing factors (difference between local observed and true ranges, uncertainties of correlation, and taxonomic noise) are assessed to determine the maximum biochronologic dating error. The local ammonite distribution data are robust in that 95% confidence level extensions of observed ranges of common ammonite taxa would not significantly modify the zonal assignment. The computer-assisted unitary association (UA) method is used for world-wide biochronologic correlation. Representative North and South American, western Tethyan, and northwest European sections were selected to establish the global maximum ranges for 103 Middle Toarcian ammonite taxa and a sequence of 40 UA. Maximum permissible correlatives of the Crassicosta Zone lie between the northwest European standard Semipolitum Subzone (late Bifrons Zone) and Bingmanni Subzone (early Thouarsense Zone). In particular, the dated tuff layer cannot be older than the Semipolitum Subzone or younger than the Illustris Subzone (Variabilis Zone). Taxonomic inconsistencies are present in the source data but their effect in corrupting UA-based correlation is shown to be negligible. The precise U–Pb age (2σ error $< \pm 1\%$) that is constrained at the (sub)zonal level furnishes a useful new time scale calibration point. It warrants adjustments to previous Toarcian stage boundary age estimates and allows a significant reduction of their associated uncertainties.

Keywords: absolute age; U/Pb; Toarcian; biochronology; calibration; Ammonites

---

[*] Corresponding author. Fax: +1 604 822 6088. E-mail: palfy@eos.ubc.ca

[1] Present address: Department of Geology, Leicester University, University Road, Leicester, LE1 7RH, UK and NERC Isotope Geoscience Laboratory, Keyworth, Notts., NG12 5GG, UK. E-mail: r.parrish@nigl.nerc.ac.uk

[2] E-mail: psmith@eos.ubc.ca

PII S0012-821X(96)00241-5

1. Introduction

The paradox of Jurassic geochronology is that the biochronologic framework was laid out in the mid 19th century [1] and has been continuously refined (see [2] for one of several recent reviews) but its calibration with isotopic ages is still poor [3]. Recently published time scales [4–12] suggest conflicting boundary age estimates and stage durations. Where uncertainties are quoted [4,9,11,12], the boundaries of the Toarcian appear the most poorly constrained of all the Jurassic stages. Underlying this problem, there is a scarcity of isotopic dates (eight items listed in [9,11,12]), of which all except one are K–Ar or Rb–Sr ages with inferior precision and accuracy. Also, most dated samples are stratigraphically poorly constrained and none of them is unambiguously confined to the Toarcian stage.

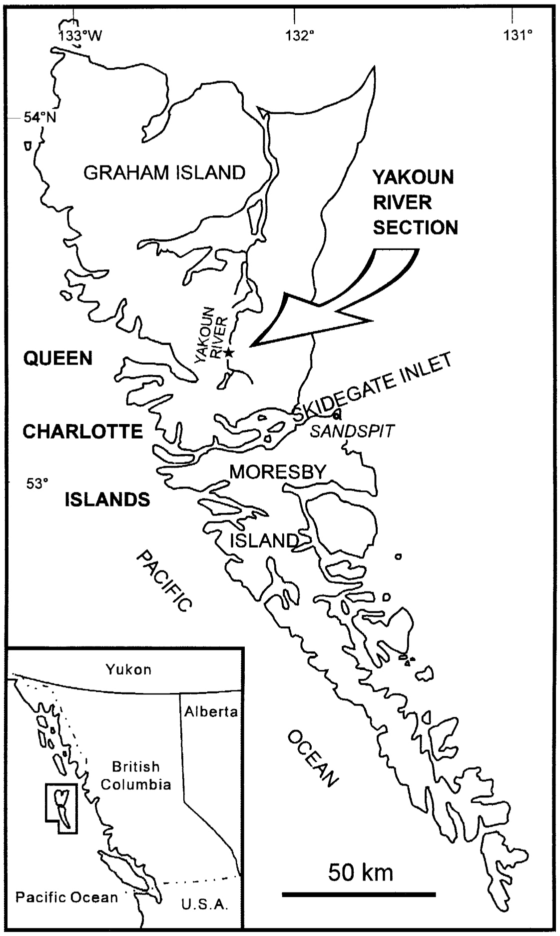

Fig. 1. Location map of the Yakoun River section on Graham Island, Queen Charlotte Islands. Grid reference for the U–Pb sample locality is UTM Zone 9, 681500E 5921830N.

To improve the calibration of the Jurassic time scale, concerted effort is under way in the Canadian Cordillera [13]. U–Pb dating of volcanic units is preferred where fossiliferous volcanosedimentary sequences allow independent ammonite biochronologic dating at the zonal level.

We report a new, precise (error is less than $\pm 1\%$ at 2σ level) U–Pb zircon age from the Queen Charlotte Islands. The dated sample is biochronologically constrained at the zonal level. Moreover, it was obtained from the type section of three consecutive Middle and Upper Toarcian North American standard ammonite zones [14]. To demonstrate the usefulness of this date as a time scale calibration point, we rigorously assess the ammonite fossil record of the section using classical confidence intervals for taxon ranges [15,16], the global biochronological correlations using the unitary association (UA) method [17], and the effect of fossil identification errors using model calculations. These methods serve to evaluate the biochronologic dating error that is not easily quantifiable. In previous time scales it was either not entered into calculations [11,12] or overestimated [9]. Conclusions derived here can be extended to the use of other dates from the North American Cordillera as calibration points for the Jurassic time scale.

2. Geologic setting

The studied section is exposed on the left bank of Yakoun River on Graham Island, Queen Charlotte Islands, British Columbia (Fig. 1). Jurassic rocks of the archipelago are assigned to Wrangellia, one of the major tectonostratigraphic terranes comprising the North American Cordillera [18]. The Jurassic stratigraphy of Wrangellia is characterized by arc-related volcanosedimentary sequences, although the Lower Jurassic Kunga and Maude groups are predominantly sedimentary on the Queen Charlotte Islands. The Yakoun River section is the designated type section of the Whiteaves Formation within the Maude Group (Section 15 in [19]). The stratigraphy of the section is shown in Fig. 2. The Whiteaves Formation consists of dark, poorly bedded concretionary mudstone with minor sandstone interbeds and rare, thin bentonitic ash layers. It records deposition in a marine basin of moderate water depth [19]. There is no apparent gap within the exposed section. The Whiteaves Formation is comformably overlain by thin-bedded to massive sandstone of the Phantom Creek Formation, although the basal part of that unit is largely concealed.

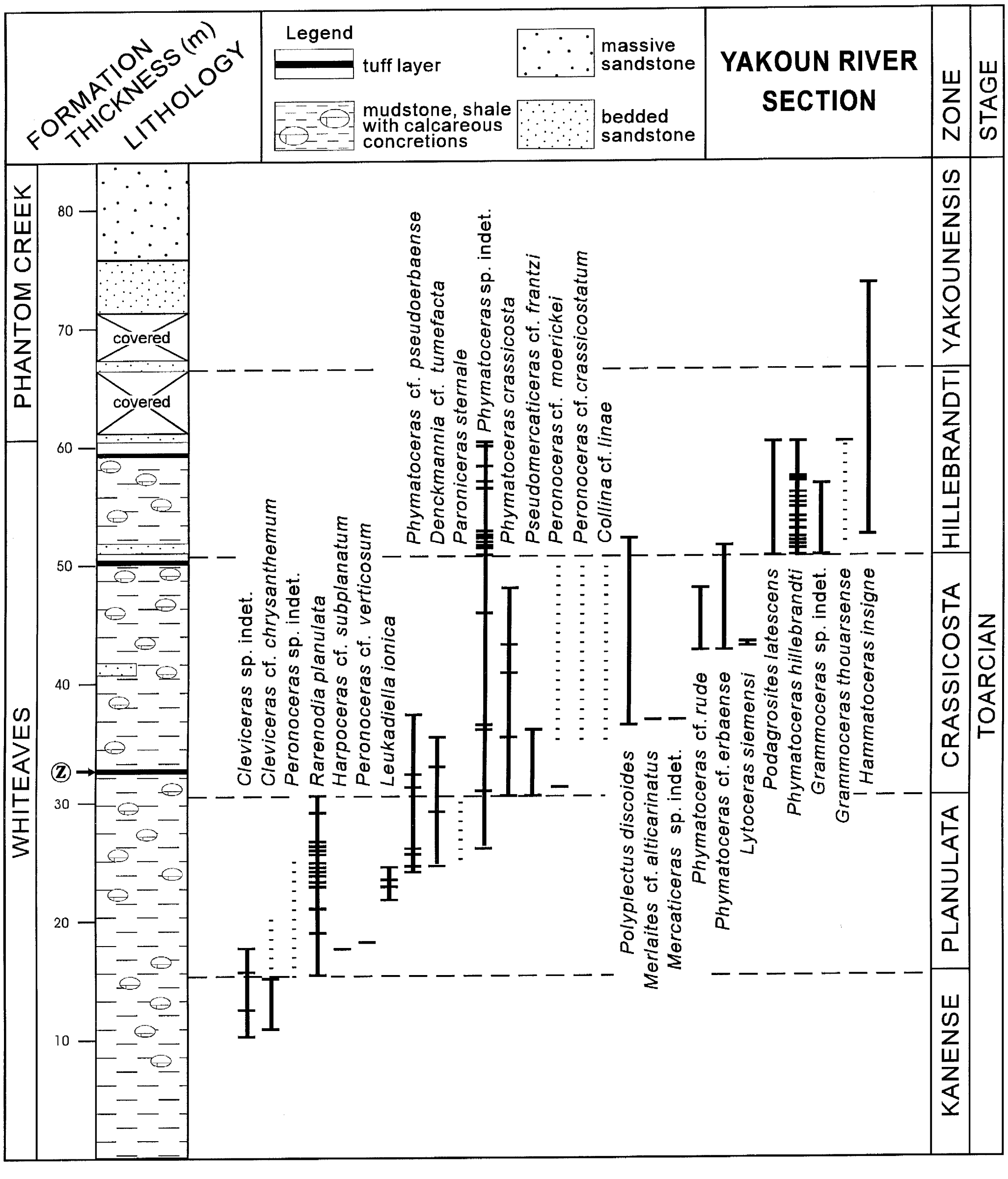

Fig. 2. Lithostratigraphy and biostratigraphy of the Toarcian of the Yakoun River section (modified after [14]). Z = the level of U–Pb zircon sample. Ammonite ranges (vertical lines) with collection levels (horizontal bars) are shown for the Planulata, Crassicosta, and Hillebrandti zones only (after [29]). Dotted lines denote imprecisely located early collections.

Table 1
U–Pb (zircon) analytical data and apparent ages from sample PCA-YR-1, a volcanic ash layer in the Whiteaves Formation at Yakoun River

Fraction [a]	Wt. [b] (μg)	U (ppm)	Pb [c] (ppm)	^{206}Pb/^{204}Pb [d]	Pb [c,e] (pg)	Th/U	^{206}Pb/^{238}U [f]	^{207}Pb/^{235}U [f]	^{207}Pb/^{206}Pb [f]	^{206}Pb/^{238}U age [g] (Ma)	^{207}Pb/^{235}U age [g] (Ma)	Corr. coef.	^{207}Pb/^{206}Pb age [g] (Ma)
A-1,s*	2.5	455.8	12.80	477	4.4	0.30	0.02854 ± 0.34	0.1973 ± 0.83	0.05014 ± 0.73	181.4 ± 1.2	182.8 ± 2.8	0.49	202 ± 34
A-4,s*	1.0	1021	28.73	113	18.9	0.32	0.02839 ± 0.32	0.1970 ± 2.56	0.05033 ± 2.39	180.5 ± 1.2	182.6 ± 8.6	0.57	210 ± 110
A-7	11.0	186.4	5.291	354	10.9	0.34	0.02853 ± 1.18	0.1980 ± 2.70	0.05034 ± 2.24	181.3 ± 4.2	183.4 ± 9.1	0.58	211 ± 104
B,s*	1.0	266.5	7.567	100	5.8	0.33	0.02862 ± 0.56	0.1842 ± 4.02	0.04668 ± 3.79	181.9 ± 2.0	171.7 ± 12.7	0.47	33 ± 182
B-3	3.7	406.9	11.71	1094	2.5	0.39	0.02853 ± 0.33	0.1947 ± 0.49	0.04948 ± 0.43	181.4 ± 1.2	180.6 ± 1.6	0.50	171 ± 20
C-2,s*	1.0	1533	42.22	393	7.2	0.25	0.02855 ± 0.40	0.1955 ± 0.97	0.04966 ± 0.86	181.4 ± 1.4	181.3 ± 3.2	0.45	179 ± 40

[a] s = single grain; * = weight estimated.

[b] Weighing error: 0.001 mg.

[c] Radiogenic Pb.

[d] Measured ratio, corrected for spike and Pb fractionation of 0.09% ± 0.03%/AMU.

[e] Total common Pb in analysis corrected for fractionation and spike.

[f] Corrected for blank Pb and U, and model common Pb composition [25] for 181 Ma Pb; errors are 1 standard error of the mean in percent.

[g] Corrected for blank and common Pb; errors are 2 standard errors of the mean in Ma.

3. U–Pb geochronometry

3.1. Methodology

Sample PCA-YR-1 was collected from a 10 cm thick, clay-rich, white gritty ash bed interbedded within black mudstone of the Whiteaves Formation in the Yakoun River section. The sample was excavated with a knife and spoon and stored in a moist state. In the laboratory the sample was blended into a slurry, allowed to settle, and the fines decanted. The washed concentrate was further ultrasonically agitated and cleaned, passed through heavy liquids, and separated into aliquots with different magnetic susceptibilities. Euhedral needles of zircon were identified in the least magnetic material, hand picked, photographed, and abraded [20] for U–Pb analysis. Crystals selected were reasonably homogeneous but, allowing for the possibility that xenocrysts or transported zircons may have been present, the first set of analyses were of single grains weighing only a few micrograms. The concordance and reproducibility of these analyses established a high probability of a single population of zircon, and additional analyses consisted of up to 10 grains to achieve somewhat smaller U–Pb analytical errors. The methods and decay constants used in U–Pb analyses are described elsewhere [21–23]. Table 1 presents these data and errors [24], and they are shown graphically in Fig. 3. U and Pb blanks were approximately 0.2 and 3 pg, respectively.

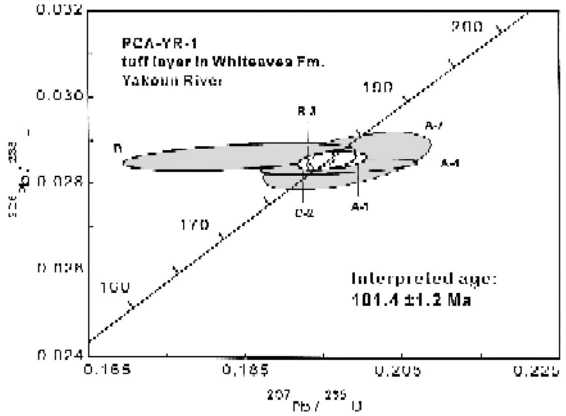

Fig. 3. U–Pb concordia diagram for zircons from sample PCA-YR-1, a volcanic ash layer in the Whiteaves Formation at Yakoun River. Errors are shown at 2σ (95%) level. Error ellipses with thick outline denote single grain analyses, grey shading indicates fractions not used in final age interpretation (see text for details and Table 1 for analytical data).

3.2. Results

Six analyses of single or multiple grains of abraded zircons all produced consistently concordant and overlapping error ellipses on the concordia diagram (Fig. 3). In Jurassic zircons the abundance ratio of $^{206}Pb/^{207}Pb$ is about 20, therefore the $^{206}Pb/^{238}U$ age from single grain analyses is inherently more precise than the $^{207}Pb/^{235}U$ age and it reliably estimates the crystallization age when concordance is demonstrated and the $^{206}Pb/^{238}U$ ages form a tight cluster [26]. The strong abrasion of the grains [20], their mutual concordance, and agreement in their $^{206}Pb/^{238}U$ ages definitively argue against any subsequent Pb loss in the crystals analyzed. The weighted mean of $^{206}Pb/^{238}U$ ages based on all six fractions is 181.2 ± 0.6 Ma (2σ). We take a more conservative approach by selecting the three most precise analyses (A-1, B-3 and C-2) and, noting their concordance, we use the mutual overlap of their $^{206}Pb/^{238}U$ ages as the best estimate of the true age and uncertainty and assign 181.4 ± 1.2 Ma (2σ) as the crystallization age of zircons and eruption of ash.

4. Biochronology

Biochronologic dating is based on sequences of associations of taxa that have been shown to maintain their stratigraphic relationships over a wide geographic area. This approach is well suited to ammonoids and has been successfully used in developing zonations for the North American Lower Jurassic [14,27]. The use of the new U–Pb date as a time scale calibration point requires correlation between the secondary standard North American and the primary standard northwest European zonations (see [28] for discussion). Here we develop such a correlation and apply additional methods to test for biochronologic error.

4.1. The ammonite fossil record

The Whiteaves Formation in the Yakoun River section is richly fossiliferous. The most common macrofossils are ammonites, with a total of 119 collections obtained through initial reconnaissance work [19], followed by three field seasons of careful systematic sampling [29]. This collection history and the abundance of fauna distinguishes the Yakoun River section as one of the best studied Early Jurassic ammonite localities in North America. Well preserved ammonites occur most commonly in non-septarian calcareous concretions, the majority of which are distributed randomly in the section, while some form distinct layers. Although rare, ammonites were also found crushed within the shale (G. Jakobs, pers. commun. 1996). The uniform lithology throughout the Whiteaves Formation suggests that there is no significant preservational bias affecting the vertical distribution of fossils, which was carefully measured and documented [14,29].

Five regional standard ammonite zones were proposed for the Toarcian of North America [14]. All of them are recognizable in the Yakoun River section, which serves as the stratotype for the Planulata, Crassicosta, and Hillebrandti zones [14]. The ash layer yielding the analyzed U–Pb sample is by definition assigned to the lower part of Crassicosta Zone. Therefore, the following discussion is concerned with the Crassicosta and the adjacent Planulata and Hillebrandti zones only.

4.2. Reliability of observed ranges

The regional standard zonal scheme for the Toarcian [14] is based on a literal reading of observed vertical ranges of ammonites. It is widely accepted, however, that the fossil record is incomplete [30] and it underestimates the true ranges [31]. Our aim in assessing the robustness of ammonite zones as defined in the Yakoun River section is twofold: to use rigorous statistical methods to test the validity of zones and to compare the empirical data derived from successive collecting campaigns with the predictions from statistical methods. The following calculations are based on published fossil occurrence data [14,29].

The simplest way of providing a maximum estimate of the completeness of the ammonite record is to calculate a ‘‘hit/miss’’ ratio, where the hits are confirmed occurrences and the misses are collection levels with no record of a given taxon within its known vertical range (also termed virtual occurrences [17]). For the 54 levels reported within the three zones, there are 74 hits and 110 misses, suggesting that the maximum average probability of finding a species in a fossiliferous horizon within its vertical range is no better than 40%. It can be argued that the average probability is biased towards lower values by rare taxa which are given little weight in devising biozonations. Of the 22 taxa considered, only six (*Rarenodia planulata*, *Phymatoceras crassicosta*, *P. hillebrandti*, *P.* cf. *pseudoerbaense*, *Leukadiella ionica*, and *Denckmannia tumefacta*) were found at more than two levels. Indeed, these six taxa score a hit/miss ratio of 51/54 giving a nearly 50% chance of being found. Not surprisingly, the three zonal index species among them score the highest (hit/miss = 36/20, chance of being found = 64%).

It is evident that misses would occur beyond the lowest and highest hits; that is, the observed ranges are shorter than the true local ranges. To estimate the true ranges, gaps separating occurrence levels must also be considered [15,30]. Fig. 2 is a re-plotting of observed ranges [14] considering all available information on vertical distribution [29]. The distribution of gap lengths in the fossil record is shown to have Dirichlet distribution and classical confidence intervals can be calculated for estimating the true stratigraphic ranges [15,16]. These statistics are only valid if the fossil distribution is assumed to be random. As pointed out above, there is no appreciable preservational bias or change in sedimentation rate in the rather uniform lithologic sequence of the Whiteaves Formation. Likewise, collection bias can also be discounted as collection intensity was constant during the first field season and collecting strategy remained systematic (although slightly biased towards parts of the Planulata and Hillebrandti zones) in the following two campaigns (G. Jakobs, pers. commun., 1996).

Extensions of the observed ranges for the six common taxa were calculated at the 95% confidence level [16] and plotted in Fig. 4. Note that the length of the range extension is a function of the length of the observed range and the number of occurrences within it. The statistical meaning of the range extensions is that there is less than 5% probability of finding a given species beyond the limits of the extended range. For the three zonal index species, occurrences are separated according to the year of their first finding and changes in cumulative observed ranges are also plotted. The following observations can be made: (1) For commonly occurring ammonite taxa collected through systematic collecting effort, range extensions at the 95% confidence are not justifiable. A lesser degree of confidence would better agree with range extensions realized through further collecting but its approximate level needs to be established empirically through tests on a larger database. (2) The Planulata, Crassicosta, and Hillebrandti zones are defined as assemblage zones [14]. In practice, the definition of their boundaries at the stratotype depends, to a large degree, on the range of their zonal index species. The Planulata and Hillebrandti zones are based on robust evidence from the distribution of their respective zonal indices. Their range extension even at the 95% confidence level would not modify the zonation significantly. The Crassicosta Zone, on the other hand, is less well defined by the range of its zonal index but is well constrained by the subjacent and superjacent zones and the cohort of co-occurring taxa. (3) Of the six range end-points of other relatively common species, only one would require modification of zonal assignments if the range extension at the 95% confidence level is considered. (4) The isotopically dated tuff layer (within the observed range of *Phymatoceras crassicosta*) falls very near to the top of the extended range (at the 95% confidence level) of *Rarenodia planulata*, therefore its assignment to the Crassicosta Zone is undoubted.

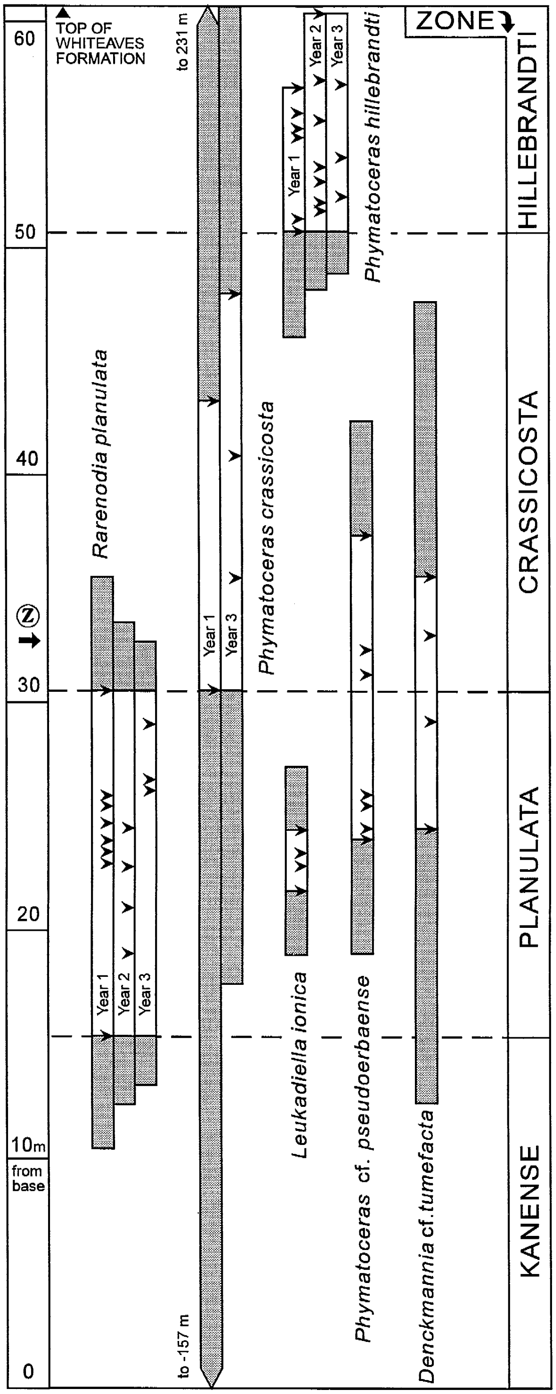

Fig. 4. Collection levels (arrowheads), observed ranges (unfilled boxes), and estimated maximum ranges at 95% confidence level (shaded boxes) of common ammonite species (i.e., occurring at more than two levels) from the Planulata, Crassicosta, and Hillebrandti zones in the Yakoun River section. Changes in observed and estimated ranges after successive collection years are shown for the three zonal index species (*Rarenodia planulata, Phymatoceras crassicosta,* and *P. hillebrandti*). Occurrence data from [29]. Z = the level of U–Pb zircon sample. See text for discussion.

4.3. Biochronologic correlations

Traditional ammonite biochronology was founded and proved extremely powerful within single bioprovinces (e.g., Boreal northwest Europe, Tethys) where it is possible to establish reproducible high resolution units (faunal horizons). Limitations and difficulties are imposed by facies dependence and limited paleobiogeographic distribution of taxa, resulting in complex time/space distribution patterns overprinted by the vagaries of fossil record (i.e., preservation and collection biases). Correlation across biogeographical boundaries is often controversial, as exemplified by long-standing debates on Tethyan/Boreal correlation in the Toarcian of Europe [32]. The traditional approach is based on expert judgement in emphasizing the correlation value of certain ammonoid taxa and their associations at the expense of others when discrepancies in the first and last appearance datums (FAD/LAD) are detected.

A traditional solution for the correlation of North American Toarcian ammonite zones with northwest European standard zones (sensu [33]) equates the Planulata Zone with the Bifrons and basal Variabilis zones, the Crassicosta Zone with the rest of the Variabilis Zone, and the Hillebrandti Zone with the Thouarsense Zone [14]. It is acknowledged that: (1) correlation is hampered by the absence of key European taxa in North American faunas (e.g., *Hildoceras* and *Haugia*, to which index species of the Bifrons and Variabilis zones belong); (2) North American faunas have greater similarity to Tethyan and South American ones than those of Boreal northwest Europe; (3) in North America, the FAD and/or LAD of several important genera (e.g., *Phymatoceras*, *Podagrosites*, *Peronoceras*, and *Mercaticeras*) are anomalous with respect to those found elsewhere [14]. Consequently, a cautious approach to correlation needs to integrate global stratigraphic distribution from all faunal provinces, should seek maximum ranges of taxa, and is expected to result in a correlation scheme with apparent resolution sacrificed for increased reproducibility and confidence. The amount of available data calls for quantitative treatment, which also provides the advantage of eliminating potential bias introduced by subjective judgements.

There is a variety of quantitative biostratigraphic techniques available and the choice depends on the nature of data and the expected outcome [34]. In our case, the data are obtained from measured sections in different sedimentary basins and bioprovinces, hence the total number of taxa is high (>100) while the number of common taxa is often low. Also, fossil distribution among sections may be non-random due to faunal migration. As the timing of migration events is not known independently, maximum ranges are sought to use for correlation. Among the most widely used and tested quantitative methods, graphic correlation seeks maximum ranges but is not practical beyond a single sedimentary basin [35]. The probabilistic ranking and scaling method also works best within a single basin/bioprovince, where it produces average ranges with the maximum likelihood of FAD/LAD sequence while assuming random distribution of fossils [36]. The unitary association (UA) method [17] appears to be best suited to our problem. It furnishes maximum ranges based on a deterministic approach and it does not require random fossil distribution or homogeneity of source data. It applies the rigor of graph theory to the familiar concept of Oppelian assemblage zones, thus it retains the philosophy underlying traditional ammonite biochronology. The pitfalls of intuitive correlation schemes are minimized. The algorithmic formulation of the UA method resulted in an efficient computer program, the BioGraph [37]. The UA method was found to efficiently construct biochronologically meaningful zonations from complex data [38]. Notably, it was successfully used for correlation between different bioprovinces [39] and was demonstrated to reproduce closely the ammonite zonation developed by traditional methods in northwest Europe [40].

We used the following procedure for computer-assisted biochronologic correlation. Conventional correlation of the Planulata, Crassicosta, and Hillebrandti zones [14] was accepted as a guide. The scanning range was set to latest Early to early Late Toarcian. All established ammonite provinces were considered and the available literature was culled for representative sections from each province. The selection was based on evidence that collections were made from measured sections spanning several zones with no indication of condensed horizons or reworking, that the ammonite fauna is abundant and diverse, and that local ranges are well documented. Sources with sound taxonomic documentation (preferably with illustration) were chosen if possible. No adequate sections meeting the above criteria were located from the western Pacific and Arctic provinces. Beside the Yakoun River section, data from one other North American, four South American, five western Tethyan and five northwest European sections were compiled (see Appendix A for details of sources and remarks). Among the taxa occurring, only species of Ammonitina reported from two or more localities were used. *Polyplectus* and *Pseudolioceras*, two long-ranging genera with little stratigraphic value, were omitted. Limited attempt was made to homogenize taxonomy (see discussion below), mainly to consider synonyms of taxa reported from the Yakoun River [29]. Composite genus ranges were added for each section to mitigate the effect of paleobiogeographic differences at the species level. A conservative generic classification scheme [41] was adopted with the exception of recognition of *Rarenodia* [29] and the combining of *Porpoceras* with *Peronoceras* to avoid confusion stemming from different opinions as to their species content. The 103 taxa and the stratigraphic ranges in each section are available as an **EPSL Online Background dataset** [3] (''appendix 2'').

These data were entered into and processed by the BioGraph program [37]. Sections within each province were ordered, with priority given to the most species-rich and complete one. As the resolution of contradictory stratigraphic relationships may be affected by the order in which the data are processed [17], all six permutations of North American, Tethyan and northwest European sections were tried with the least informative South American sections consistently entered last. The output of 40 successive UA (Fig. 5), however, was not sensitive to the permutation.

The UA assigned to specific beds or collection levels in the source sections were determined from the correlation tables produced by BioGraph (available as **EPSL Online Background Dataset**, ''appendix 3''). Thus, at the Yakoun River, the base of the Crassicosta Zone corresponds to UA 22-23, the base of the Hillebrandti Zone to UA 33, and the isotopically dated tuff layer to UA 22-25. Standard subzonal and zonal boundaries reported from the analyzed northwest European sections were used to determine the maximum permissible extent of these units in terms of the UA scheme (Fig. 6). (Lacking a universally accepted Toarcian standard zonation for northwest Europe, we adopt a recently updated scheme [32] which differs only slightly from a more traditional zonation [33]. Notably, the subzones of the Bifrons Zones are based on the species sequence of *Hildoceras*, the Variabilis Zone is subdivided into three subzones, and the subzonal scheme within the Thouarsense Zone is revised, increasing the correlation potential [32].) The most likely range, as expressed by the overlap or minimum required range of UA from the analyzed sections, was also inferred for the standard units. It is evident from Fig. 6 that individual UA are seldom reproducible in more than one or two sections and across bioprovinces. However, their groupings, which correspond to traditional zones or subzones, are commonly present in several sections from different provinces. Only four UA are unambiguously identifiable in North America and they are not directly correlatable with other provinces.

Fig. 6 is used to determine the most likely and the maximum permissible correlations of the Crassicosta Zone (and the isotopically dated level within it) with the northwest European standard zonation. The beginning of the zone appears equivalent or marginally older (but cannot be younger) than that of the standard Variabilis Subzone (Variabilis Zone). It could also be correlative with (but not older than) the later part of Semipolitum Subzone (Bifrons Zone). The beginning of Hillebrandti Zone lies most likely within the latest Variabilis Zone (Vitiosa Subzone) but it could be as old as the Illustris Subzone (middle part of Variabilis Zone) or as young as the earliest Bingmanni Subzone of the Thouarsense Zone. The isotopically dated tuff layer is constrained to the Semipolitum through Illustris subzones (inclusive), with the earlier part of the Variabilis Zone being its most likely age.

As expected, the quality of UA based correlation decreases towards either end of the scanning range (i.e., earliest Bifrons Zone and latest Thouarsense Zone) where there is insufficient superpositional control deduced from the raw data. With this caveat, the correlative of the base of Planulata Zone (UA 7-14) appears to lie somewhere between the late Sublevisoni and early Semipolitum subzones (Bifrons Zone). The top of Hillebrandti Zone (UA 38) shows robust correlation with the Thouarsense Subzone but correlation with any of the subzones (Bingmanni through Fallaciosum) of the Thouarsense Zone is permitted.

---

[3] http://www/elsevier/nl/locate/epsl (mirror site USA, http://www.elsevier.com/locate epsl)

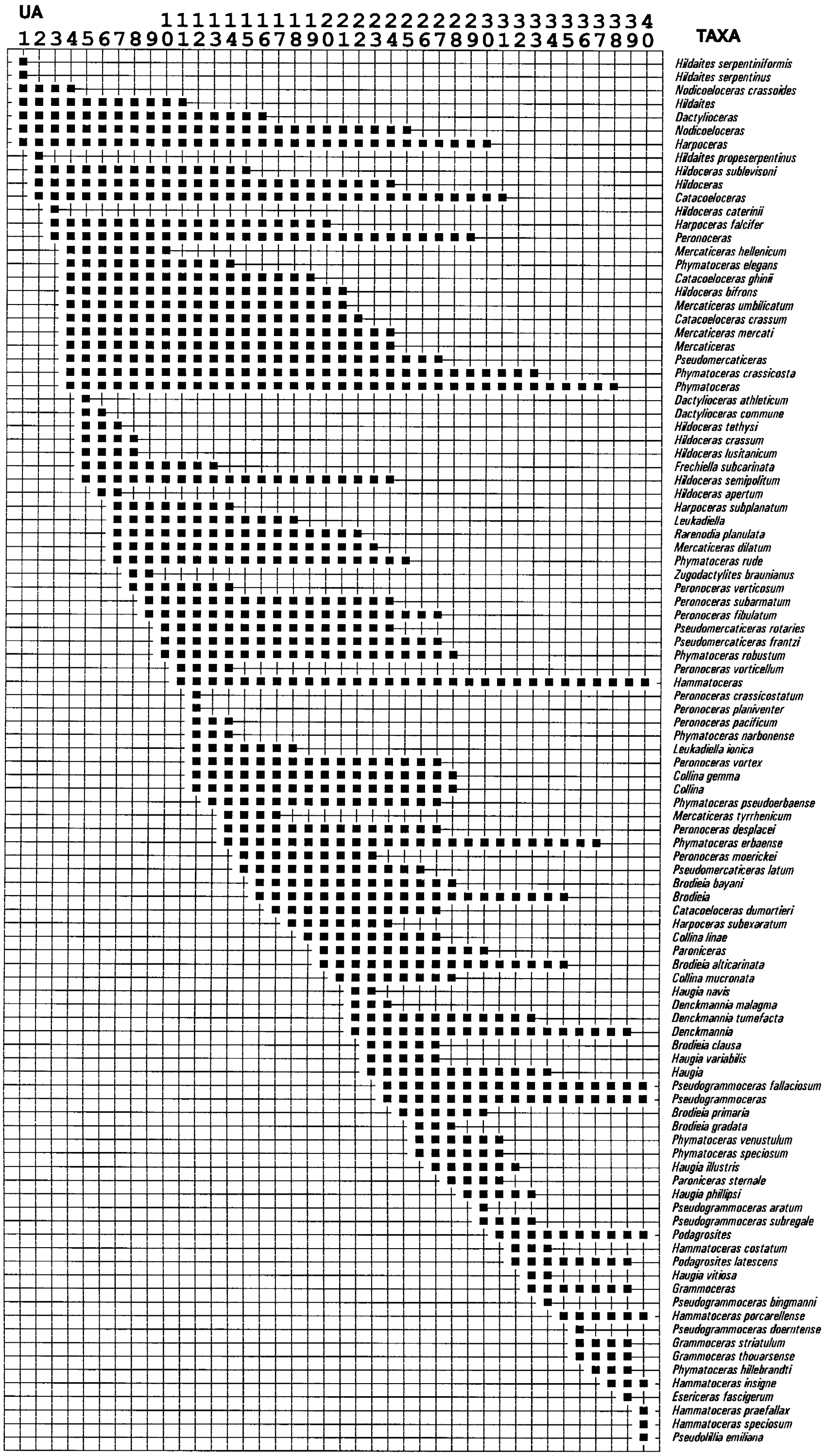
UA
1 2 3 4 5 6 7 8 9 10 11 12 13 14 15 16 17 18 19 20 21 22 23 24 25 26 27 28 29 30 31 32 33 34 35 36 37 38 39 40
TAXA
Hildaites serpentiniformis
Hildaites serpentinus
Nodicoeloceras crassoides
Hildaites
Dactylioceras
Nodicoeloceras
Harpoceras
Hildaites propeserpentinus
Hildoceras sublevisoni
Hildoceras
Catacoeloceras
Hildoceras caterinii
Harpoceras falcifer
Peronoceras
Mercaticeras hellenicum
Phymatoceras elegans
Catacoeloceras ghinii
Hildoceras bifrons
Mercaticeras umbilicatum
Catacoeloceras crassum
Mercaticeras mercati
Mercaticeras
Pseudomercaticeras
Phymatoceras crassicosta
Phymatoceras
Dactylioceras athleticum
Dactylioceras commune
Hildoceras tethysi
Hildoceras crassum
Hildoceras lusitanicum
Frechiella subcarinata
Hildoceras semipolitum
Hildoceras apertum
Harpoceras subplanatum
Leukadiella
Rarenodia planulata
Mercaticeras dilatum
Phymatoceras rude
Zugodactylites braunianus
Peronoceras verticosum
Peronoceras subarmatum
Peronoceras fibulatum
Pseudomercaticeras rotaries
Pseudomercaticeras frantzi
Phymatoceras robustum
Peronoceras vorticellum
Hammatoceras
Peronoceras crassicostatum
Peronoceras planiventer
Peronoceras pacificum
Phymatoceras narbonense
Leukadiella ionica
Peronoceras vortex
Collina gemma
Collina
Phymatoceras pseudoerbaense
Mercaticeras tyrrhenicum
Peronoceras desplacei
Phymatoceras erbaense
Peronoceras moerickei
Pseudomercaticeras latum
Brodieia bayani
Brodieia
Catacoeloceras dumortieri
Harpoceras subexaratum
Collina linae
Paroniceras
Brodieia alticarinata
Collina mucronata
Haugia navis
Denckmannia malagma
Denckmannia tumefacta
Denckmannia
Brodieia clausa
Haugia variabilis
Haugia
Pseudogrammoceras fallaciosum
Pseudogrammoceras
Brodieia primaria
Brodieia gradata
Phymatoceras venustulum
Phymatoceras speciosum
Haugia illustris
Paroniceras sternale
Haugia phillipsi
Pseudogrammoceras aratum
Pseudogrammoceras subregale
Podagrosites
Hammatoceras costatum
Podagrosites latescens
Haugia vitiosa
Grammoceras
Pseudogrammoceras bingmanni
Hammatoceras porcarellense
Pseudogrammoceras doerntense
Grammoceras striatulum
Grammoceras thouarsense
Phymatoceras hillebrandti
Hammatoceras insigne
Esericeras fascigerum
Hammatoceras praefallax
Hammatoceras speciosum
Pseudolillia emiliana

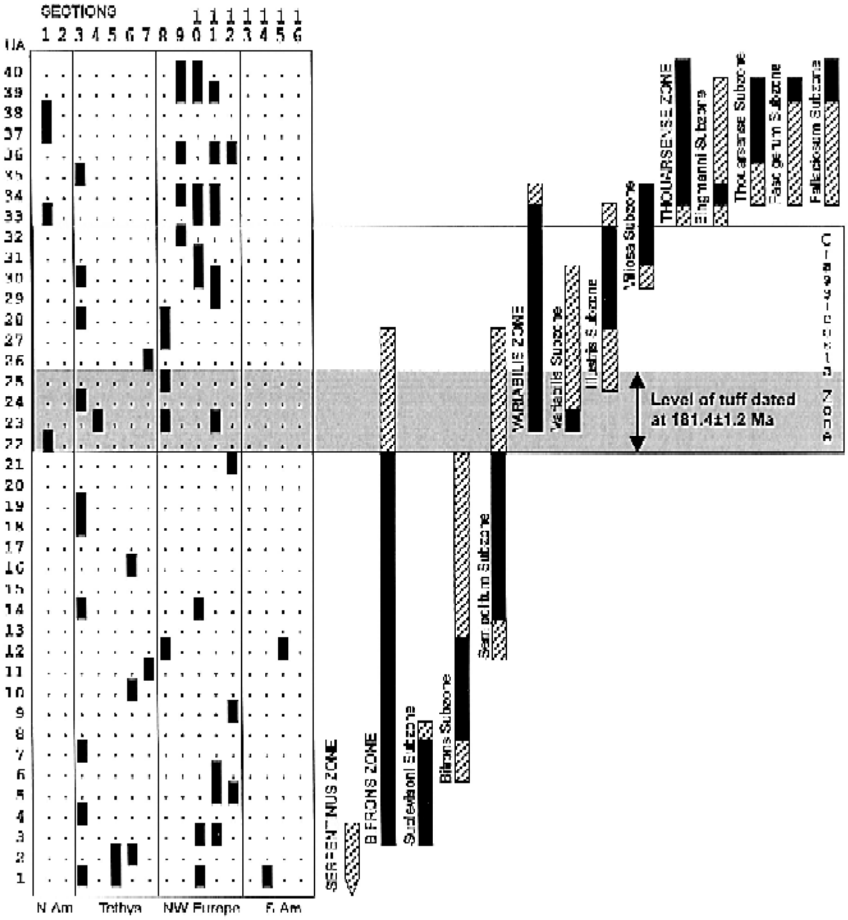

Fig. 6. Reproducibility of the 40 Unitary Associations recognized in latest Early to early Late Toarcian ammonite faunas analyzed using the BioGraph program. The left side of diagram shows the occurrences of UA (solid bars) in the 16 selected sections (listed in Appendix A). Plotted on the right side are minimal (solid bars) and maximal (hatched bars) groupings of UA corresponding to the northwest European standard zones and subzones [32] and their correlation with the North American Crassicosta Zone (box) and the isotopically dated level (gray shaded) within it.

4.4. The effect of taxonomic noise

In addition to differences between observed and true fossil ranges and correlation uncertainty, a third potential source of error in biochronologic dating is the uncertainty of fossil identification. Given the variety of authors and their differing opinions on species, taxonomic noise (i.e., random inconsistencies in identifications) is expected in the source data for biochronologic correlation. The following example is given to illustrate the effect of high levels of taxonomic noise.

The stratigraphically important genus *Hildoceras* was recently revised [42]. Four widely distributed species were accepted with many other nominal species synonymized (Table 2). Tabulated are the revisions made to figured specimens from sources used in our correlation database [43–47]. In approxi-

Fig. 5. Global latest Early to early Late Toarcian ammonoid taxon ranges relative to the 40 Unitary Associations produced by the BioGraph program.

Table 2
Synonyms of species of *Hildoceras* figured in sources used in our biochronologic correlation database [43–47], as recognized in the revision of Howarth [42]

Hildoceras laticosta Bellini	*H. lusitanicum* Meister		*H. bifrons* (Bruguiere)		*H. semipolitum* Buckman
(= *H. sublevisoni* Fucini; *H. caterinii* Merla)	(= *H. graecum* Renz; *H. crassum* Mitzopoulos; *H. tethysi* Géczy)		(= *H. apertum* Gabilly)		(= *H. angustisiphonatum* Prinz; *H. semicosta* Buckman)
H. graecum sublevisoni [43]	? ***H. semipolitum*** [43]	↔	***H. semipolitum*** [43]		*H. semipolitum* [45]
? ***Hildaites levisoni*** [44]	*H. graecum graecum* [43]		***H. semicosta*** [45]	↔	*H. semicosta* [45]
H. sublevisoni [46]	*H. graecum lusitanicum* [43]		*H. bifrons* [45]		*H. angustisiphonata* [45]
H. sublevisoni [47]	***H. sublevisoni*** [44]		*H. bifrons* [46]	↔	***H. bifrons*** [46]
H. caterinii [47]	***H. sublevisoni*** [45]		*H. apertum* [46]		*H. bifrons* var. *angustisiphonata* [46]
	? *H. graecum* [45]		*H. bifrons bifrons* [43]		
	? *H. lusitanicum* [45]		*H. bifrons walcoti* [43]		*H. semipolitum* [46]
	H. lusitanicum [46]		*H. bifrons bifrons* [44]		*H. semipolitum* [47]
	H. tethysi [47]		***H. bifrons angustisiphonatum*** [44]		
	H. crassum [47]		***H. semipolitum*** [44]		
	H. lusitanicum [47]		*H. apertum* [47]		
			H. bifrons [47]		

Subjective junior synonyms are given in parentheses in the heading [42]. Bold face indicates disagreement between the reviser and the original author after reassignment of synonymized nominal species. Arrows mark specimens originally figured under one name that are now assigned to two different species [42].

mately 25% of the cases, the original author's identification is revised in addition to reassignments of synonymized nominal species. In three cases, specimens originally figured under one name are assigned to two different species by the reviser. It follows that, even with amply illustrated material, the stratigraphic distribution data cannot be unambiguously revised without a comprehensive review of all considered specimens, a daunting task not attempted here.

If we adopt this high figure of 25% erroneous identifications at the species level, we can then examine the effect of this taxonomic noise on the UA correlation method. The simplest model calculation is to construct UA from two species (A and B), both represented by one specimen at two levels of a hypothetical stratigraphic section (Fig. 7). The stratigraphic ranges of A and B can be concurrent, overlapping, or exclusive. There is a single UA in case of concurrent or overlapping ranges whereas two successive UA are identified for exclusive ranges. Let one specimen; that is, one quarter of the total, be misidentified (A erroneously called B or B called A). In each case, there are four permutations to place the misidentified specimens. Recording the changes in UA and the proportion of number of levels with erroneously assigned UA provides a measure of sensitivity of the UA method to taxonomic noise. We shall only consider the critical errors where the misidentification leads to the addition of artificial UA or to a shift of UA boundary. If the result is the merger of two UA, the net effect is a decrease in resolution and loss of correlation power without introduction of correlation error.

As shown in Fig. 7, there are two permutations for the overlapping ranges and two for the exclusive ranges where a total of five levels suffer critical error in UA assignment. A comparison with the total number of levels considered in all scenarios (36) reveals that at the 25% taxonomic noise level, the critical stratigraphic error is less than 14%. A remarkable property of the UA method is that increase in the density or complexity of source data greatly reduces the sensitivity to taxonomic noise. In the model calculation, it can be demonstrated that a twofold increase in the number of occurrence levels (from two to four) leads to less than 3% critical stratigraphic error at the same 25% taxonomic noise level. Furthermore, we note that misidentification most often occurs among morphologically similar forms that are often phylogenetically closely related and have similar stratigraphic distributions. Taxonomic mistakes involving taxa with concurrent ranges will not introduce stratigraphic error. The amount and complexity of data used in the world-wide correlation, together with the foregoing considerations, lead us to regard the contribution of taxonomic noise to biochronologic dating error as negligible.

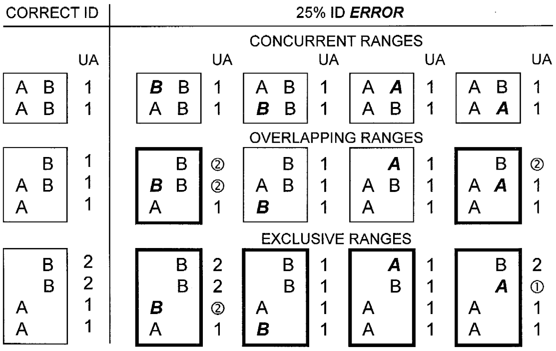

Fig. 7. Simulation of the effect of 25% taxonomic noise on the unitary associations (UA). Left column: stratigraphic relationships of species A and B known from two levels in each section and derived UA. Other four columns: permutations of one misidentified specimen (in bold italic type). Heavy border denotes modification in UA pattern compared with left column, circled UA number denotes levels of critical error. See text for discussion.

5. Discussion

The results of the correlation using the UA method can be compared with those obtained traditionally [14]. The boundary of Planulata and Crassicosta zones, previously correlated with the early part of Variabilis Zone, is now allowed to fall within the interval of Semipolitum to Variabilis subzones, with the greatest likelihood indeed near the base of the Variabilis Zone. The boundary of Crassicosta and Hillebrandti zones, previously equated with the base of the Thouarsense Zone, is now allowed to fall within the interval of Illustris Subzone to the base of Thouarsense Zone, most likely within the Vitiosa Subzone.

As demonstrated above, the maximum uncertainty in biochronologic age assignment of the isotopically

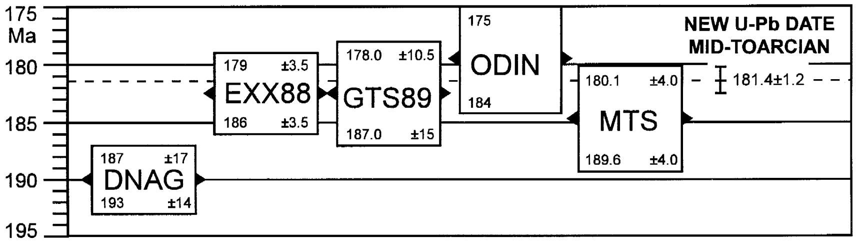

Fig. 8. Comparison of boundary age estimates and numerical mid-point (marked with arrowheads) of the Toarcian in some recent time scales and the new U–Pb date from the mid-Toarcian of Queen Charlotte Islands. Sources of time scales quoted: DNAG [4–6]; EXX88 [7,8]; GTS89 [9]; Odin [10]; MTS [11,12].

dated sample is ± 1 standard subzone. It is superior to all previously available dates, which are constrained at the stage level at best. The precision of the U–Pb age also surpasses that of any other isotopic age from, or near, the Toarcian. Thus the U–Pb age from near the middle of Middle Toarcian at Yakoun River serves as an important new calibration point for the Jurassic time scale. When plotted against the major recently published and widely used time scales, the new U–Pb date of 181.4 ± 1.2 Ma falls within the Toarcian in all except the DNAG [4–6] scale (Fig. 8). The mid-point of Toarcian is within the error of our date in the EXX88 [7,8] and GTS89 [9] scales only. The new date is significant in that it, together with other newly obtained Early Jurassic isotopic ages, will help greatly reduce the large uncertainty associated with previous stage boundary estimates. Rigorous error estimates are only given in GTS89 [9] and MTS [11,12]. Considering the error ranges, in GTS89 [9] the base of the Toarcian can be as young as 172 Ma and the top as old as 188.5 Ma, both outside the error limits of the new U–Pb date. In MTS [11,12], the top of the Toarcian can be as old as 184.1 Ma, which is in conflict with the U–Pb date reported here.

6. Conclusions

We report a newly obtained U–Pb zircon age of 181.4 ± 1.2 Ma (2σ) from the Queen Charlotte Islands. The interpreted age is based on concordant and overlapping analyses of single-crystal as well as multi-grain fractions. The dated sample was collected from a bentonitic ash layer within the Toarcian Whiteaves Formation in the Yakoun River section. The ash layer lies within the North American standard Crassicosta Zone as defined by ammonite biostratigraphy [14].

The Yakoun River is the designated type section of the Crassicosta Zone as well as the subjacent Planulata and superjacent Hillebrandti zones [14]. We statistically analyzed the quality of the ammonite fossil record in this section. All three zones are assemblage zones by definition but, in practice, are delimited at the stratotype by their respective index species. The collection density of *Rarenodia planulata* and *Phymatoceras hillebrandti* is adequate in that their range extension using 95% confidence intervals would not modify the placement of the zonal boundaries significantly. Collection data from three successive field seasons [29] suggest that generally much less than 95% confidence level is required when proposing range extensions for commonly occurring ammonite taxa. The assignment of the dated tuff layer to the lower part of Crassicosta Zone would not change even when range extensions at the 90% confidence level are considered.

Biochronologic correlation was done using the computer-assisted unitary association (UA) method [17]. Ammonite local range data from representative North American, western Tethyan, northwest European, and South American sections were processed to provide unbiased estimates of global maximum taxon ranges and a sequence of UA. The UA framework was then used to establish the maximum extent of permissible correlation between the secondary standard North American and the primary standard northwest European zonations. Correlation of the Crassicosta Zone is bracketed by the Semipolitum Subzone (late Bifrons Zone) and Bingmanni Subzone (early Thouarsense Zone). In particular, the dated tuff layer cannot be older than the Semipolitum Subzone or younger than the Illustris Subzone (Variabilis Zone).

Random misidentifications are known to occur in the world-wide dataset used for correlation. However, the UA method is shown to respond to taxonomic noise by loss of resolution rather than erroneous correlation. Thus we regard the proposed correlation as conservative best estimates.

With less than ±1% (2σ) error in the isotopic age and a maximum of ±1 standard subzone uncertainty in biochronologic correlation, the U–Pb age from the Yakoun River section serves as an important calibration point for the Early Jurassic time scale. A comparison with recently proposed time scales reveals that only minor adjustments are required for the Toarcian stage boundary age estimates but the associated uncertainties can be greatly reduced. U–Pb dating of volcanic horizons within fossiliferous sequences in the North American Cordillera holds promise for providing more useful calibration points for the Jurassic time scale.

Acknowledgements

Giselle Jakobs is thanked for sharing her extensive knowledge of the Yakoun River locality and Toarcian ammonite faunas in general, answering our many questions, and allowing access to her unpublished data. Anne Kinsman provided expert assistance in producing a heavy mineral concentrate and in aspects of U–Pb chemistry. Klaus Santowski performed expert mass spectrometry on these tiny zircon samples. Thoughtful comments by James Ogg, Robert Anderson, and an anonymous reviewer helped improve the manuscript. Financial support through an NSERC grant to PLS and a Killam pre-doctoral fellowship to JP is gratefully acknowledged. ***[RV]***

Appendix A. List of stratigraphic sections and sources of BioGraph input

A.1. North America

(1) Yakoun River, British Columbia [14,29]

(2) Joan Lake, British Columbia [14,29]

A.2. Western Tethys

(3) Valdorbia, Umbria, Italy [44,48] (As bed-by-bed correlation between the two sources are ambiguous at some levels, data from the two sources was first processed by BioGraph and the resulting taxa ranges with UA treated as levels were entered into the main BioGraph input file.)

(4) Djebel-es-Saffeh (Section 3B), Djebel Nador area, Algeria [46]

(5) Djebel-es-Saffeh (Section 2), Djebel Nador area, Algeria [46] (Supplementary section to Djebel-es-Saffeh 3B, mainly to better document the ammonite fauna from the lower part of the succession.)

(6) Paghania, Greece [43]

(7) Monte di Civitella, Umbria, Italy [49]

A.3. Northwest Europe

(8) St-Paul des Fonts, Aveyron, France [45] (Ammonite faunas of horizons, said to represent one to three beds, are given and entered here as levels.)

(9) Camplong, Aveyron, France [50]

(10) Ricla and La Almunia, Iberian Range, Spain [51]

(11) Anse Saint-Nicolas, Vendée, France [47] (From the vicinity of Thouars, the classical type area for the Toarcian, this section contains the best documented and most diverse ammonoid fauna.)

(12) Ravenscar and Whitby, Yorkshire, England [42,52,53] (Data compiled following the bed-by-bed correlation between the two sections [42].)

A.4. South America

(13) Quebrada El Bolito, northern Chile [54]

(14) Quebrada Yerbas Buenas, northern Chile [54]

(15) Quebrada Larga, northern Chile [54]

(16) Rio del Toro, northern Chile [54] (For all South American sections emended taxonomy was used [55].)

References

[1] A. Oppel, Die Juraformation Englands, Frankreichs und südwestlichen Deutschlands, 857 pp., Ebner & Seubert, Stuttgart, 1856–1858.

[2] S.S. Buckman and J.H. Callomon, Time from fossils: Juras-

sic high-resolution geochronology, in: Milestones in Geology, M.J. Le Bas, ed., Geol. Soc. London Mem. 16, 127–150, 1995.

[3] J. Pálfy, Development of the Jurassic geochronologic scale, Hantkeniana 1, 13–25, 1995.

[4] A.R. Palmer, The Decade of the North American Geology 1983 geologic time scale, Geology 11, 503–504, 1983.

[5] D.V. Kent and F.M. Gradstein, A Cretaceous and Jurassic geochronology, GSA Bull. 96, 1419–1427, 1985.

[6] D.V. Kent and F.M. Gradstein, A Jurassic to recent chronology, in: The Western North Atlantic Region, P.R. Vogt and B.E. Tucholke, eds., The Geology of North America, M, pp. 45–50, GSA, Boulder, CO, 1986.

[7] B.U. Haq, J. Hardenbol and P.R. Vail, Chronology of fluctuating sea levels since the Triassic, Science 235, 1156–1167, 1987.

[8] B.U. Haq, J. Hardenbol and P.R. Vail, Mesozoic and Cenozoic chronostratigraphy and cycles of sea level change, SEPM Spec. Publ. 42, 71–108, 1988.

[9] W.B. Harland, R.L. Armstrong, A.V. Cox, L.E. Craig, A.G. Smith and D.G. Smith, A Geologic Time Scale 1989, 263 pp., Cambridge Univ. Press, Cambridge, 1990.

[10] G.S. Odin, Geological time scale, C.R. Acad. Sci. Ser. 2 318, 59–71, 1994.

[11] F.M. Gradstein, F.P. Agterberg, J.G. Ogg, J. Hardenbol, P. van Veen, J. Thierry and Z. Huang, A Mesozoic time scale, J. Geophys. Res. B 99, 24,051–24,074, 1994.

[12] F.M. Gradstein, F.P. Agterberg, J.G. Ogg, J. Hardenbol, P. van Veen, J. Thierry and Z. Huang, A Triassic, Jurassic, and Cretaceous time scale, in: Geochronology, Time Scales and Global Stratigraphic Correlation, W.A. Berggren, D.V. Kent, M.-P. Aubry and J. Hardenbol, eds., SEPM Spec. Publ. 54, 95–126, 1995.

[13] J. Pálfy, P.L. Smith, J.K. Mortensen, R.M. Friedman, V.J. McNicoll, R.R. Parrish and R.G. Anderson, Progress on Cordilleran Jurassic time scale calibration, Geol. Assoc. Can. Progr. Abs. 20, A-79, 1995.

[14] G.K. Jakobs, P.L. Smith and H.W. Tipper, An ammonite zonation for the Toarcian (Lower Jurassic) of the North American Cordillera, Can. J. Earth Sci. 31, 919–942, 1994.

[15] M. Springer and A. Lilje, Biostratigraphy and gap analysis; the expected sequence of biostratigraphic events, J. Geol. 96, 228–236, 1988.

[16] C.R. Marshall, Confidence intervals on stratigraphic ranges, Paleobiology 16, 1–10, 1990.

[17] J. Guex, Biochronological Correlations, 252 pp., Springer, Berlin, 1991.

[18] J.W.H. Monger, J.O. Wheeler, H.W. Tipper, H. Gabrielse, T. Harms, L.C. Struik, R.B. Campbell, C.J. Dodds, G.E. Gehrels and J. O'Brien, Cordilleran terranes, in: Upper Devonian to Middle Jurassic assemblages, in: Geology of the Cordilleran Orogen in Canada, H. Gabrielse and C.J. Yorath, eds., Geology of Canada 4 (also The Geology of North America G-2), pp. 281–327, Geol. Surv. Can. (also GSA), 1991.

[19] B.E.B. Cameron and H.W. Tipper, Jurassic stratigraphy of the Queen Charlotte Islands, British Columbia, Geol. Surv. Can. Bull. 365, 1–49, 1985.

[20] T.E. Krogh, Improved accuracy of U–Pb zircon ages by the creation of more concordant systems using an air abrasion technique, Geochim. Cosmochim. Acta 46, 637–649, 1982.

[21] R.R. Parrish, J.C. Roddick, W.D. Loveridge and R.W. Sullivan, Uranium–lead analytical techniques at the geochronology laboratory, Geological Survey of Canada, Geol. Surv. Can. Pap. 87-2, 3–7, 1987.

[22] J.C. Roddick, W.D. Loveridge and R.R. Parrish, Precise U–Pb dating of zircon at the sub-nanogram Pb level, Chem. Geol. Isot. Geosci. Sect. 66, 111–121, 1987.

[23] R.H. Steiger and E. Jäger, Subcommission on geochronology: Convention on the use of decay constants in geo- and cosmochronology, Earth Planet. Sci. Lett. 36, 359–362, 1977.

[24] J.C. Roddick, Generalized numerical error analysis with applications to geochronology and thermodynamics, Geochim. Cosmochim. Acta 51, 2129–2135, 1987.

[25] J.S. Stacey and J.D. Kramers, Approximation of terrestrial lead isotope evolution by a two-stage model, Earth Planet. Sci. Lett. 26, 207–221, 1975.

[26] R. Mundil, P. Brack, M. Meier, H. Rieber and F. Oberli, High resolution U–Pb dating of Middle Triassic volcaniclastics: Time-scale calibration and verification of tuning parameters for carbonate sedimentation, Earth Planet. Sci. Lett. 141, 137–151, 1996.

[27] P.L. Smith, H.W. Tipper, D.G. Taylor and J. Guex, An ammonite zonation for the Lower Jurassic of Canada and the United States: the Pliensbachian, Can. J. Earth Sci. 25, 1503–1523, 1988.

[28] J.H. Callomon, Biostratigraphy, chronostratigraphy and all that — again!, in: Int. Symp. on Jurassic Stratigraphy, Erlangen, O. Michelsen and A. Zeiss, eds., pp. 611–624, Geol. Surv. Den., 1984.

[29] G.K. Jakobs, Toarcian ammonite faunas from the North American Cordillera, Geol. Surv. Can. Bull. 428, in press, 1997.

[30] C.R.C. Paul, The adequacy of the fossil record, in: Problems of Phylogenetic Reconstruction, K.A. Joysey and A.E. Friday, eds., Syst. Assoc. Spec. Vol. 21, 75–117, 1982.

[31] P.W. Signor and J.H. Lipps, Sampling bias, gradual extinction patterns and catastrophes in the fossil record, in: Geological Implications of Impacts of Large Asteroids and Comets on the Earth, L.T. Silver and P.H. Schiltz, eds., GSA Spec. Pap. 190, 291–296, 1982.

[32] S. Elmi, J. Gabilly, R. Mouterde, L. Rulleau and R.B. Rocha, L'étage Toarcien de l'Europe et de la Téthys; Divisions et correlations, Geobios Mém. Spéc. 17, 149–159, 1994.

[33] W.T. Dean, D.T. Donovan and M.K. Howarth, The Liassic ammonite zones and subzones of the northwest European province, Bull. Brit. Mus. Nat. Hist. Geol. 4, 438–505, 1961.

[34] L.E. Edwards, Quantitative biostratigraphy: The method should suit the data, in: Quantitative Stratigraphic Correlation, J.M. Cubitt and R.A. Reyment, eds., pp. 45–60, Wiley, Chichester, 1982.

[35] K.O. Mann and H.R. Lane, Graphic Correlation, 263 pp., SEPM, Tulsa, OK, 1995.

[36] F.P. Agterberg, Automated Stratigraphic Correlation, 424 pp., Elsevier, New York, NY, 1990.

[37] J. Savary and J. Guex, BioGraph: un nouveau programme de construction des corrélations biochronologiques basées sur les associations unitaires, Bull. Géol. Lausanne 313, 317–340, 1991.

[38] P.O. Baumgartner, Comparison of unitary associations and probabilistic ranking and scaling as applied to Mesozoic radiolarians, Comput. Geosci. 10, 167–183, 1984.

[39] P.O. Baumgartner, Early Cretaceous radiolarians of the Northeast Indian Ocean (Leg 123: Sites 765, 766 and DSDP site 261): The Antarctic–Tethys connection, Mar. Micropaleontol. 21, 329–352, 1993.

[40] J.-L. Dommergues and C. Meister, La biostratigraphie des ammonites du Carixien (Jurassique inférieur) d'Europe occidentale: un test de la méthode des associations unitaires, Eclog. Geol. Helv. 80, 919–938, 1987.

[41] D.T. Donovan, J.H. Callomon and M.K. Howarth, Classification of the Jurassic Ammonitina, in: The Ammonoidea, M.R. House and J.R. Senior, eds., Syst. Assoc. Spec. Publ. 18, 101–155, 1981.

[42] M.K. Howarth, The ammonite family Hildoceratidae in the Lower Jurassic of Britain, Palaeontogr. Soc. Monogr. London 145–146, Publ. No. 586 and 590, 1–200, 1992.

[43] A.V. Kottek, Die Ammonitenabfolge des griechischen Toarcium, Ann. Géol. Pays Hell. 17, 1–157, 1966.

[44] M.F. Gallitelli Wendt, Ammoniti e stratigrafia del Toarciano umbro-marchigiano (Appennino centrale), Boll. Soc. Paleontol. Ital. 8, 11–62, 1970.

[45] J. Guex, Répartition biostratigraphique des ammonites du Toarcien moyen de la bordure sud des Causses (France) et révision des ammonites décrites et figurées par Monestier (1931), Eclog. Geol. Helv. 65, 611–645, 1972.

[46] S. Elmi, F. Atrops and C. Mangold, Les zones d'ammonites du Domérien–Callovien de l'Algérie occidentale — Première partie: Domérien–Toarcien, Docum. Lab. Géol. Fac. Sci. Lyon 61, 1–84, 1974.

[47] J. Gabilly, Le Toarcien à Thouars et dans le centre-ouest de la France, 217 pp., Centre Natl. Rech. Sci., Paris, 1976.

[48] S. Cresta, G. Pallini and F. Venturi, Jurassic ammonite assemblages in the Valdorbia section, Mem. Descr. Carta Geol. Ital. 39, 89–94, 1989.

[49] F. Venturi, Rapporti filetici e stratigrafici dei generi toarciani *Mercaticeras*, *Brodieia*, *Hildoceras*, *Phymatoceras*, *Chartronia* dell'Appennino Centrale, Riv. Ital. Paleontol. Stratigr. 81, 195–246, 1975.

[50] J. Guex, Description biostratigraphique du Toarcien supérieur de la bordure sud des Causses (France), Eclog. Geol. Helv. 68, 97–129, 1975.

[51] A. Goy and G. Martínez, Biozonación del Toarciense en el área de La Almunia de Doña Godina-Ricla (Sector Central de la Cordillera Ibérica), Cuad. Geol. Iber. 14, 11–53, 1990.

[52] W.T. Dean, Notes on part of the Upper Lias succession at Blea Wyke, Yorkshire, Proc. Yorkshire Geol. Soc. 29, 161–179, 1954.

[53] M.K. Howarth, The Jet Rock Series and the Alum Shale Series of the Yorkshire Coast, Proc. Yorkshire Geol. Soc. 33, 381–422, 1962.

[54] A. von Hillebrandt and R. Schmidt-Effing, Ammoniten aus dem Toarcium (Jura) von Chile (Südamerika), Zitteliana 6, 1–74, 1981.

[55] A. von Hillebrandt, Liassic ammonite zones of South America and correlations with other provices, with descriptions of new genera and species of ammonites, in: Biostratigrafia de los Sistemas Regionales del Jurásico y Cretácico en América del Sur 1, pp. 111–157, Mendoza, 1987.